JOURNAL OF COMMUNICATIONS AND INFORMATION SYSTEMS, VOL. 31, No. 1, MARCH 2016.

Dual-Band and Dual-Polarized Microstrip Antenna with Isolated Ports for Applications on HAPs

Lucas S. Pereira, Marcos V. T. Heckler and Cleiton Lucatel

***Abstract*—This paper presents the design of a dual-band microstrip antenna with dual polarization characteristic for high altitude platforms (HAPs). The antenna has two isolated ports and is suitable for terminals with receiving and transmitting functions operating simultaneously. The element is designed for operation at 5.8 and 7 GHz with 100 MHz bandwidth in each band. The antenna geometry and its main design parameters are presented and discussed in the paper. Numerical and experimental results show that this radiator exhibits good performance in terms of impedance matching and circular polarization purity.**

***Index Terms*—Dual-Band Antenna, Dual-Polarized Antenna, Microstrip Antenna.**

I. Introduction

MICROSTRIP and printed antennas have been used widely in wireless systems such as wireless local access network (WLAN), mobile communications and global positioning satellite systems (GNSS).

Among other advantages, microstrip antennas are very suitable for integration into arrays and can be easily integrated with discrete components, such as low-noise amplifiers, mixers and filters, which are interesting traits for the development of all variations of adaptive antennas [1]. As a special case, retro-directive antenna arrays exhibit the ability to resend signals to the same direction where they have been received from [2]. Traffic control and collision avoidance systems are examples in which retro-directive antenna arrays find future application [3], [4].

Dual-band antennas have been studied widely. The most used techniques are stacking of patches [5]-[7] and coplanar configurations [8]-[9]. However, none of these contributions analyze antennas with two isolated ports, which is the main contribution reported in this paper. The proposed antenna should be suitable for integration into a retro-directive array to be installed on a high-altitude platform (HAP). For this purpose, it should exhibit dual-band and dual-polarized behavior. Additionally, it should work as a receiving (Rx) and transmitting (Tx) antenna simultaneously. For this reason, the proposed geometry presents two ports with large isolation between them. According to the European regulations for fixed satellite systems (ECA Table) [10], the HAP should be designed to work as Rx at 5.8 GHz and as Tx at 7.0 GHz. At both frequencies, the signal to be retransmitted has maximum bandwidth of 100 MHz, which means 1.72% bandwidth at 5.8 GHz and 1.43% at 7.0 GHz. Dual polarization is used to improve isolation between the uplink and the downlink channels, whereby the antenna should be right-handed circularly polarized (RHCP) at 5.8 GHz and left-handed circularly polarized (LHCP) at 7.0 GHz [11].

In the next section, the geometry of the proposed antenna is depicted. In the section III, the parametric analysis about the decoupling stubs and the impedance matching stubs is discussed. Section IV presents the experimental validation of the built prototype.

II. Dual-Band and Dual-Polarized Microstrip Antenna

The stack-up considered for the construction of the designed antenna is shown in Figure 1. The multilayer structure is composed of three low-loss microwave laminates TACONIC TLA-6 with dielectric constant of 2.62 and loss tangent of 0.0012. The top laminate supports the patch that is tuned to operate in the higher band, whereas the radiator that resonates at 5.8 GHz is printed on the middle laminate. An air layer has been added between the patches in order to increase the bandwidth in the top band and to allow soldering the via to the bottom patch prior to the final assembly. The two lower laminates are glued with TACONIC FastRise 27 prepreg with thickness h_{glue} = 0.21 mm, dielectric constant of 2.75 and loss tangent of 0.0014. Both patches have the shape of a square with truncated corners and are fed by two independent microstrip lines. The connection between the patches and the lines is done by means of metallic vias.

The Associate Editors coordinating the review of this manuscript and approving it for publication were Prof. Cecílio José Lins Pimentel and Prof. Marcelo da Silva Pinho. A preliminary version of this paper was presented in XXXIII Simpósio Brasileiro de Telecomunicações (SBrT'15), Juiz de Fora, MG, Brazil, September 1-4, 2015 [11].

Lucas Santos Pereira, is with Universidade Federal do Pampa, Alegrete, RS, Brazil (e-mail: lucaspereira@unipampa.edu.br).

Marcos Vinicio Thomas Heckler, is with Universidade Federal do Pampa, Alegrete, RS, Brazil (e-mail: marcos.heckler@ unipampa.edu.br).

Cleiton Lucatel, is with Universidade Federal do Pampa, Alegrete, RS, Brazil (e-mail: cleiton.lucatel@unipampa.edu.br).

Digital Object Identifier: 10.14209/jcis.2016.8

The schematic top view of the antenna is shown in Figure 2. In order to avoid electrical connection between both patches, a hole was drilled in the bottom patch to isolate it from the via that feeds the top patch. The position of this hole can be changed in order to allow good axial ratio and impedance matching for the upper band of the antenna. The axial ratio for both radiators can be optimized for the desired frequencies by adjusting the side lengths L_{sup} and L_{inf} and the truncation dimensions x_{sup} and x_{inf} for the top and bottom patches, respectively.

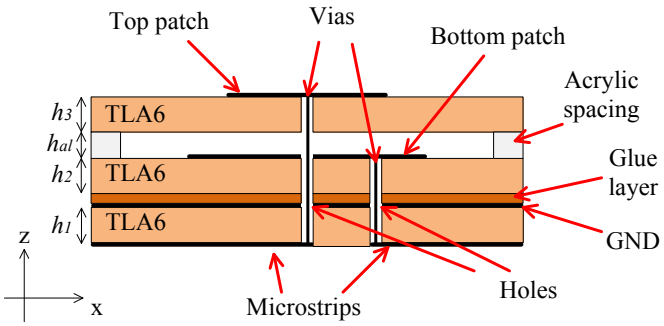

Fig. 1. Cross sectional view of the dual-band antenna.

The impedance matching for the proposed antenna cannot be realized only by adjusting the parameters y_{sup} and y_{inf} as it is the case of ordinary square patches with truncated corners. This is mainly due to the interaction between both patches, which disturbs the input impedance in comparison to single patches and due to the long via that connects the top patch to its respective feed line. In the present case, impedance matching is achieved with the open-ended single stub technique. The schematic view of the antenna feeding system is shown in Figure 3. The parameters d_{inf} and l_{inf} can be optimized to perform impedance matching at the lower band of operation (port 1). Similarly, d_{sup} and l_{sup} can be used for impedance matching at the upper band (port 2).

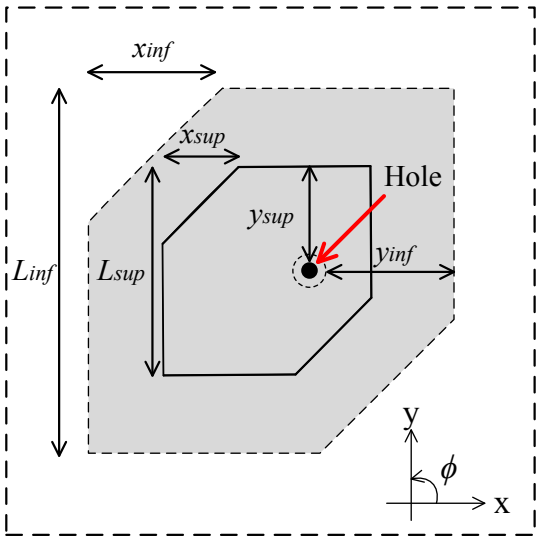

Fig. 2. Schematic top view of the two square patches.

The feeding system of the proposed radiator has two ports, as depicted in Figure 3. This antenna can be modeled as a 2x2 S–Matrix. The S_{11} parameter represents the reflection coefficient seen at port 1 when the port 2 is terminated with a matched load. Similarly, S_{22} is the reflection coefficient at port 2 when port 1 is terminated with matched load. The S_{12} and S_{21} parameters are equal, due to reciprocity, and represent the transmission coefficient between the ports [12].

In order to improve isolation between the ports, a quarter-wave open-ended stub tuned at 5.8 GHz has been connected to the line that feeds the top patch. By transmission line theory, one can derive that this stub acts as a short circuit at 5.8 GHz in the location of its connection to the feed line. As a result, the magnitude of the reflection coefficient is nearly 0 dB at this frequency, hence producing large isolation between the ports. In the top band, this quarter-wave long stub introduces an additional inductive reactance in the antenna input impedance, which needs to be taken into account during the impedance matching procedure. In the same way, a quarter-wave long stub tuned at 7.0 GHz was connected to the feed line that feeds the bottom patch. Short circuit is produced at 7.0 GHz and an additional capacitive reactance is introduced in the input impedance at 5.8 GHz. Thus the dimensions d_{bot}, l_{bot}, d_{top} and l_{top} for the two decoupling stubs must be properly chosen for the antenna to operate with two highly isolated ports.

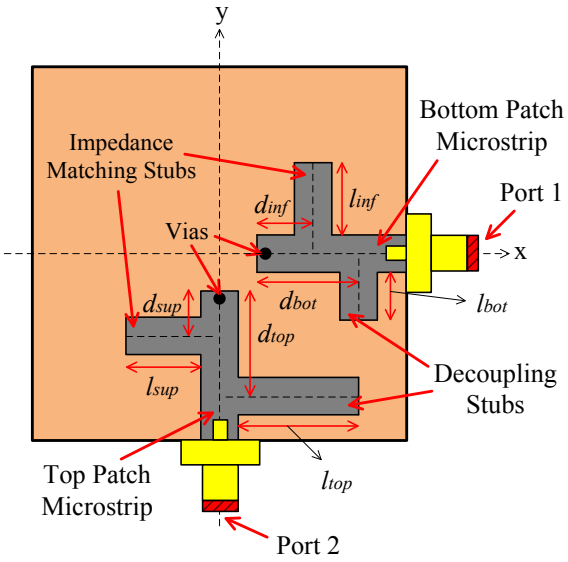

Fig. 3. Schematic view of the antenna feeding system.

III. Parametric Analysis of the Antenna

In order to investigate the radiation characteristics of the antenna, a parametric study was carried out considering changes in its dimensions. The results have been obtained with the electromagnetic simulator Ansys HFSS [13].

Firstly, variations in the two matching stubs dimensions are considered. The Figures 4 and 5 show the S-parameters considering some values of the matching stub inserted in the

bottom patch microstrip. The continuous curves represent d_{inf} = 8.4 mm, the curve with squares are for d_{inf} = 8 mm and circles are for d_{inf} = 8.8 mm in Figure 4. In the Figure 5, the continuous curves represent l_{inf} = 6.5 mm, the curve with squares are for l_{inf} = 6.1 mm and triangles are for l_{inf} = 6.9 mm.

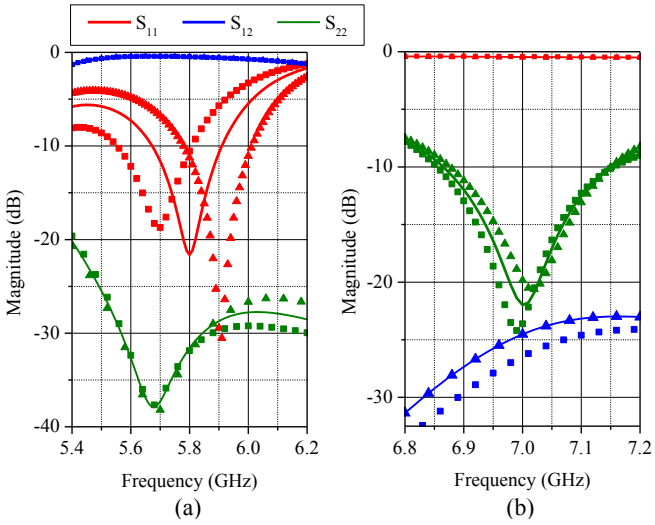

Fig. 4. Parametric analysis for the distance of the matching stub to the via in the bottom feed line.

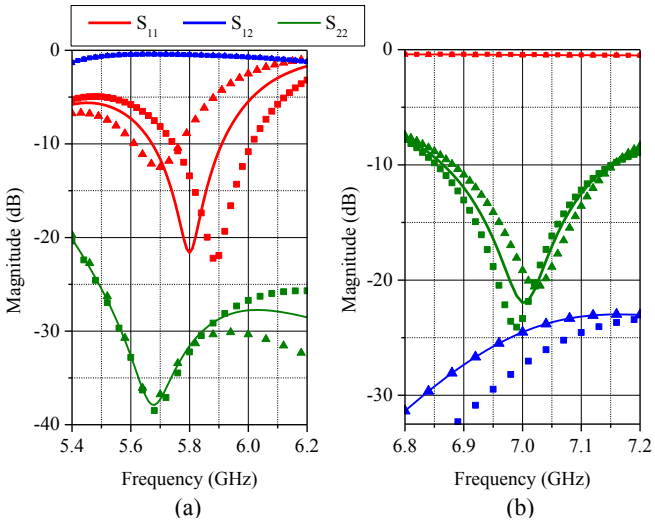

Fig. 5. Parametric analysis for the length of the matching stub in the bottom feed line.

Figures 6 and 7 show the S-parameters considering variation of the matching stub inserted in feed line for the top patch. The continuous curves represent d_{top} = 8.1 mm, the curve with square symbols are for d_{top} = 7.7 mm and circles are for d_{top} = 8.5 mm for Figure 6. In Figure 7, the continuous curves represent l_{top} = 4.6 mm, the curve with square symbols are for l_{top} = 4.2 mm and triangles are for l_{top} = 5.0 mm.

After analyzing Figures 4-7, one can verify that the parameters d_{inf} and l_{inf} only affect strongly the lower band, whereas d_{top} and l_{top} are relevant especially for the top band. This behavior is verified due to the high isolation between the two ports.

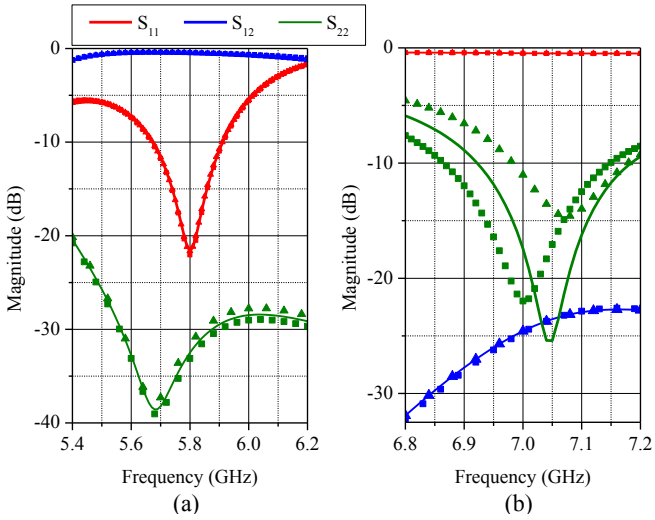

Fig. 6. Parametric analysis for the distance of the matching stub to the via in the top feed line.

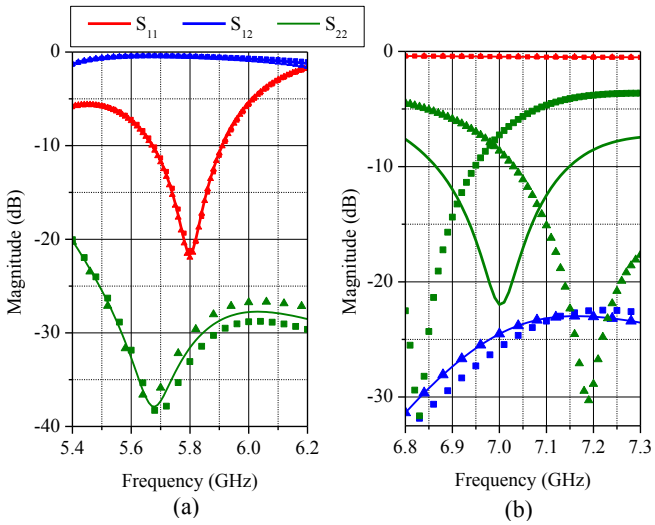

Fig. 7. Parametric analysis for the length of the matching stub in the top feed line.

Then, variations in the two decoupling stubs dimensions are considered. Figure 8 shows the S-parameters considering different values for the length of the decoupling stub inserted in the feed line for the bottom patch. The continuous curves represent l_{bot} = 6.5 mm, the curve with square symbols are for l_{bot} = 6.1 mm and circles are for l_{bot} = 6.9 mm. The S-parameters for different lengths for the decoupling stub inserted in the feed line for the top are shown in Figure 9. The continuous curves represent l_{top} = 8.4 mm, the curve with square symbols are for l_{top} = 8.0 mm and triangles are for l_{top} = 8.8 mm.

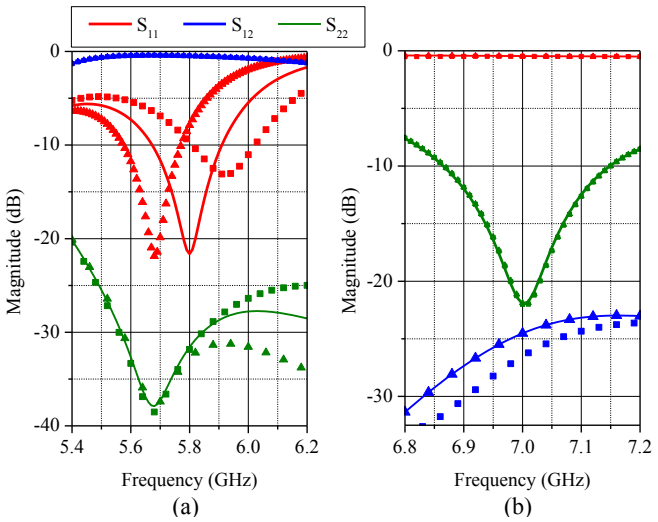

Fig. 8. Parametric analysis for the length of the decoupling stub in the bottom feed line.

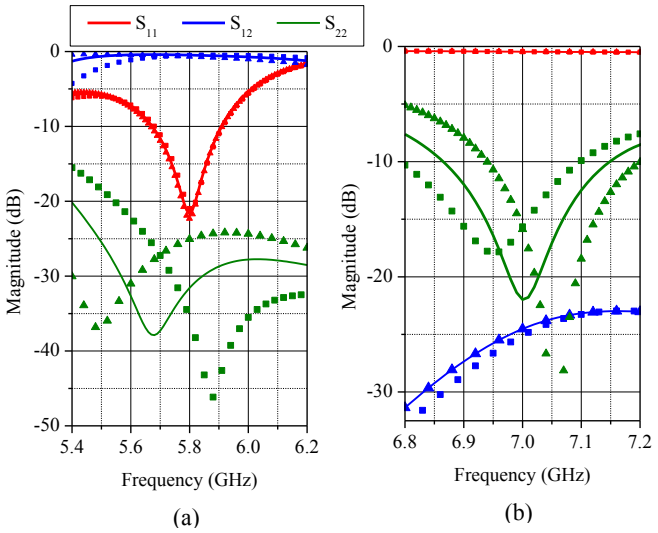

Fig. 9. Parametric analysis for the length of the decoupling stub in the top feed line.

Analyzing the behavior of the S-parameters considering variations in the decoupling stub lengths, one can say that the stub inserted in the microstrip port 1 has a strong effect in the S_{12} at the upper band (relative to port 2). However, this stub has been viewed as an additional impedance in the band centered at 7 GHz, as shown in Figure 8. Similar behavior occurs for the decoupling stub inserted in the microstrip connected to port 2.

Parametric simulations were performed in order to investigate possible deviations in the radius of the hole r_{hole} inserted in the bottom *patch*. In this case, only the axial ratio at the higher band is affected, as it is shown in Figure 10. This effect occurs because the hole may disturb the electromagnetic fields distribution in the antenna structure, especially in the top *patch* fields.

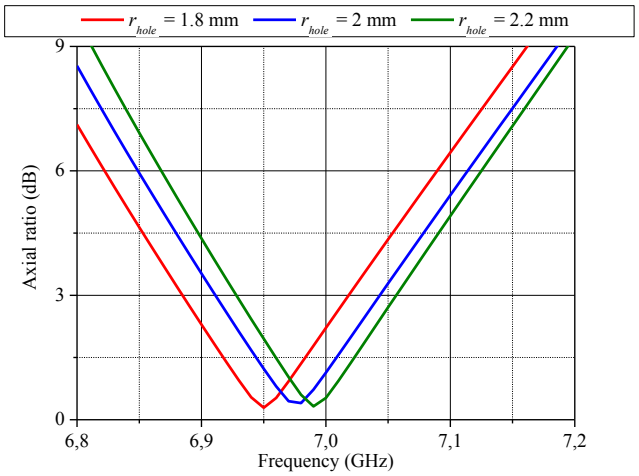

Fig. 10. Parametric analysis for the hole in the bottom patch.

IV. Experimental Characterization

A prototype was built and is shown in Figure 11. The comparison between simulated and measured S–parameters is shown in Figures 12 and 13 for the lower and higher bands, respectively. One can see that large isolation between the Rx and Tx ports is obtained, as well good impedance matching. Generally, good agreement between the simulated and experimental results has been verified.

TABLE I
Optimized Antenna Dimensions.

Parameter	Value (mm)	Parameter	Value (mm)
L_{sup}	13.63	h_3	1.96
y_{sup}	2.90	d_{inf}	8.50
x_{sup}	2.49	l_{inf}	4.50
L_{inf}	15.11	W_s	2.82
y_{inf}	5.00	d_{sup}	8.40
x_{inf}	5.63	l_{sup}	6.50
d_{hole}	2.00	d_{bot}	12.00
h_1	1.02	l_{bot}	6.50
h_2	1.96	d_{top}	10.00
W_i	2.82	l_{top}	8.40
h_{al}	1.40	h_{glue}	0.21

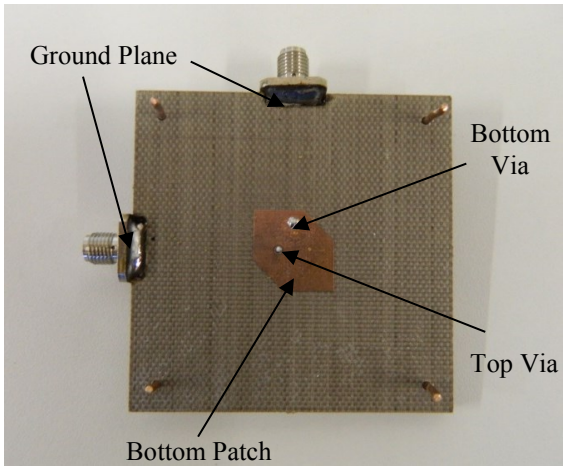

(a)

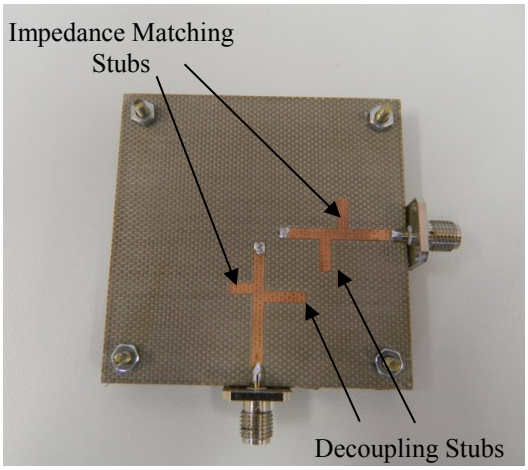

(b)

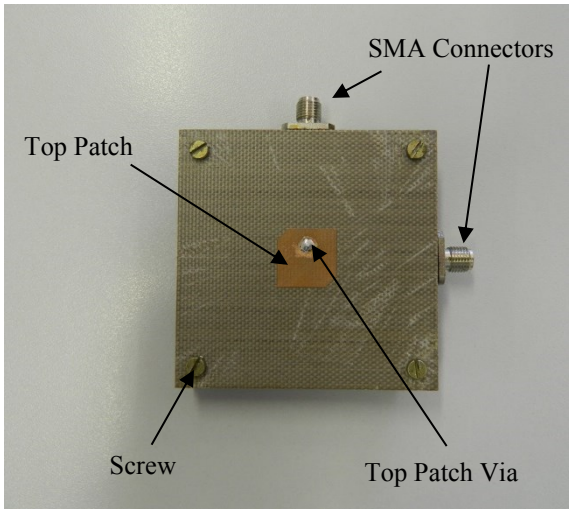

(c)

Fig. 11. Dual-band and dual-polarized microstrip antenna: (a) Top view of the bottom patch prior to the final assembly; (b) Bottom view with the feeding system of the built antenna; (c) Top view of the top patch.

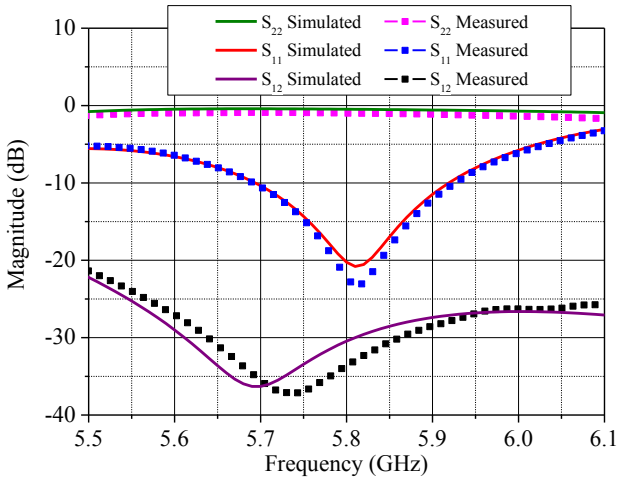

Fig. 12. Simulated and measured S-parameters in the lower band (the curves for S_{12} and S_{21} are coincident due to reciprocity).

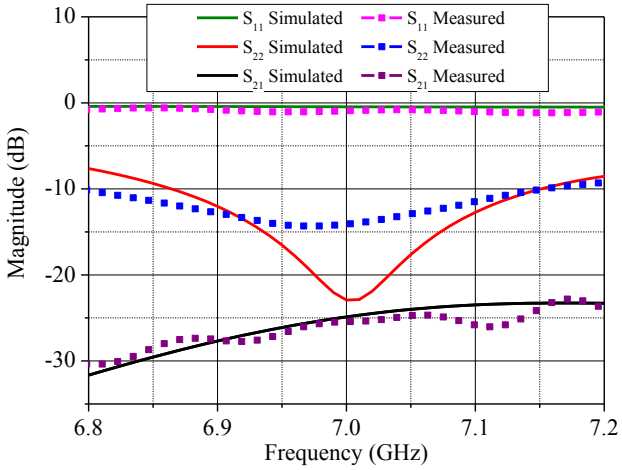

Fig. 13. Simulated and measured S-parameters in the upper band (the curves for S_{12} and S_{21} are coincident due to reciprocity).

In order to verify the deviation between the measured and simulated curves for the S_{22}-Parameter in the upper band, a parametric study was carried out by varying the thickness of the air layer. This simulates possible inaccuracy during the fabrication of the acrylic pieces used to separate the top and bottom patches, since gluing was not performed with high-precision equipment. The results are shown in Figure 14. One can see the tendency to fit the measured resonance frequency with the variation of the air layer.

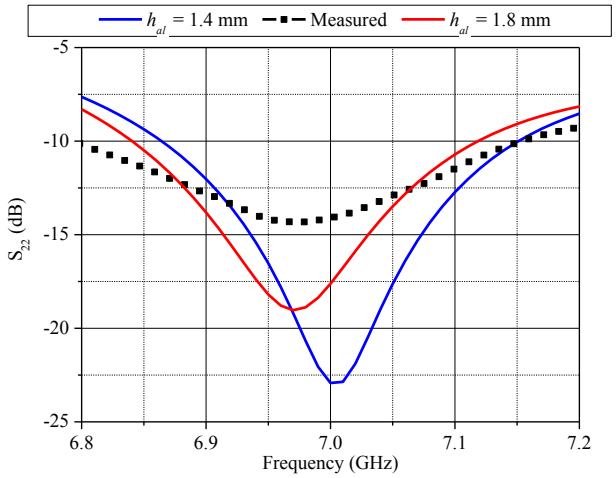

Fig. 14. Simulated and measured S_{22}-parameter in the upper band.

The comparison between the experimental results and the predicted radiation properties with HFSS at the lower and the higher bands are shown in Figures 15-19. The behavior of the axial ratio (AR) in the boresight and in the lower band has only a slight deviation from the simulated curve and the desired AR bandwidth from 5.75 to 5.85 was achieved, if the criterion AR < 3 dB is considered. For the higher band, the measured axial ratio did not fulfill the specification for the range between 6.95 and 7.05 GHz. The antenna exhibits gain in the boresight of 5.67 dBi for the lower band and 3.94 dBi for the higher band.

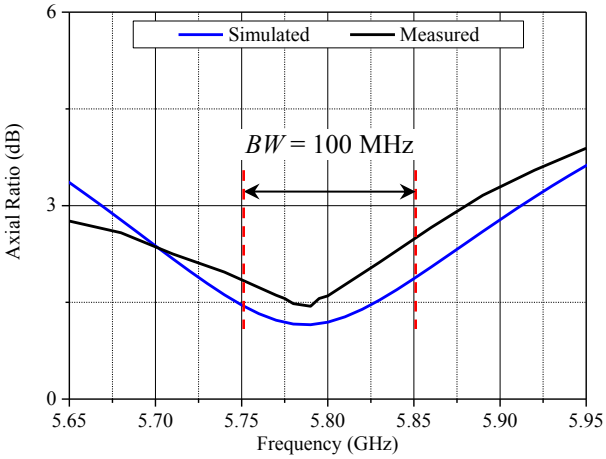

Fig. 15. Simulated and measured axial ratio in the boresight versus frequency for the lower band.

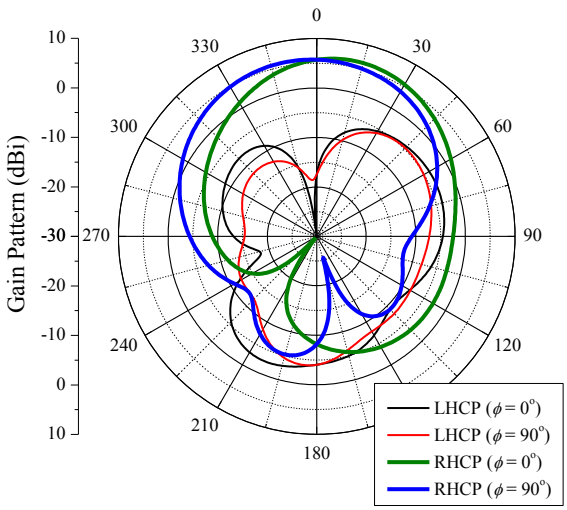

Fig. 16. Gain pattern at 5.8 GHz.

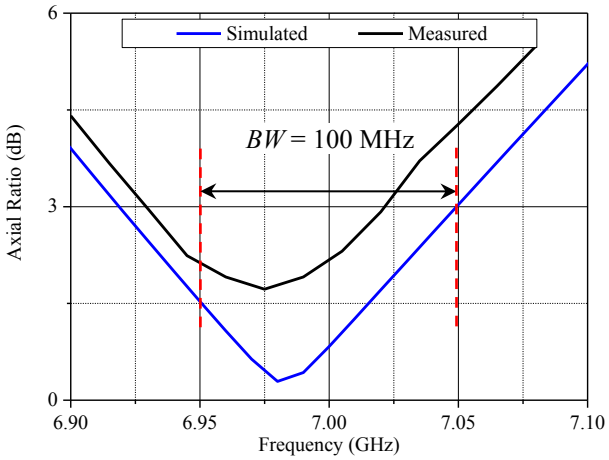

Fig. 17. Simulated and measured axial ratio in the boresight versus frequency for the upper band.

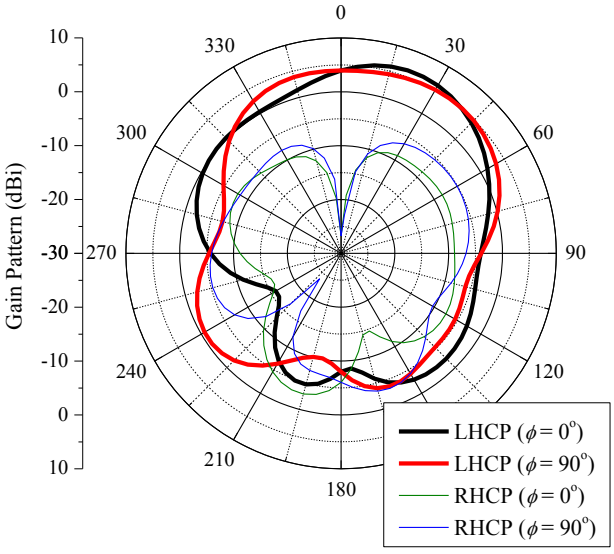

Fig. 18. Gain pattern at 7 GHz.

In order to investigate if the laminate stack-up process was done correctly, parametric analysis was performed considering displacements between both patches in x (Δ_x) and y (Δ_y) directions, as shown in Figure 19. The simulated results indicate that the experimental curve is closely reproduced if a displacement Δ_x = 0.0 mm Δ_y = -0.5 mm (red curve) is considered. This misalignment between the patches is due to the tolerances in the fabrication process, which is very critical especially at high frequencies.

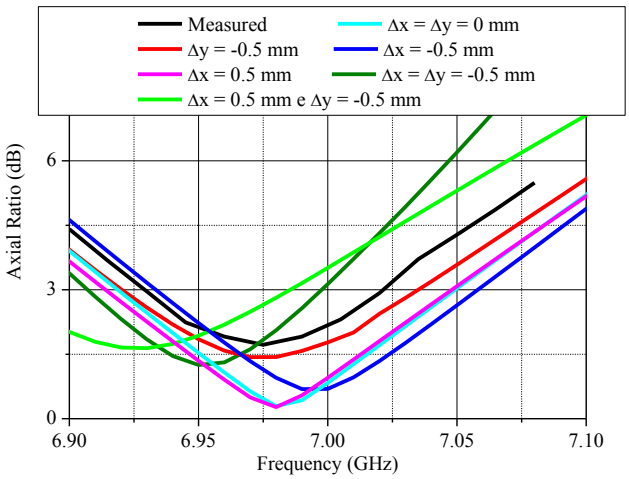

Fig. 19. Behavior of axial ratio considering misalignment between the laminates for the upper band.

V. Conclusion

This paper presented the design procedure and experimental validation of a microstrip antenna that can be operated simultaneously in two bands with circular polarization in both bands. Good agreement between measured and simulated S-parameters has been obtained.

The antenna feed system is composed of two decoupling stubs to provide the high isolation between the bands of operation and two single stubs open-ended to realize the impedance matching of the radiator. Two vias were employed to connect the two patches to the microstrips.

Large isolation between the Rx and Tx ports has been obtained experimentally. Considering the center frequencies only, the isolation is -30.5 dB at 5.8 GHz and -25 dB at 7.0 GHz. This proves that the proposed antenna concept serves as a diplexer and as a first filtering device between the Tx and Rx channels. This feature reduces strongly the requirements of filtering out the Tx band by the front-end circuitry of the receiver. Therefore, the proposed antenna is a strong candidate to compose an antenna array for high altitude platforms, since good radiation characteristics have been obtained along with good isolation between the two bands of operation.

Acknowledgments

The authors would like to thank to the National Research and Development Council (CNPq) for the partial support under grant 484406/2012-4.

References

[1] R. Garg, P. Bhartia, I. Bahl, A. Ittipiboon, “Microstrip Antenna Design Handbook”, Artech House, 2001.

[2] R. Y. Miyamoto and T. Itoh, “Retrodirective arrays for wireless communications,” IEEE Microwave Magazine, vol. 3, no. 1, pp. 71-79, Mar. 2002. doi: http://dx.doi.org/10.1109/6668.990692.

[3] C. Shyh-Jong and K. Chang. “A Retrodirective Microstrip Antenna Array”. IEEE Transactions on Antennas and Propagation, Vol. 46, No. 12, December 1998, pp. 1802-1809. doi: http://dx.doi.org/10.1109/8.743816.

[4] L. Kevin M. K. H., M. Ryan Y. and I. Tatsuo. “Moving Forward in Retrodirective Antenna Arrays”. IEEE Potentials. August/September 2003. doi: http://dx.doi.org/10.1109/MP.2003.1232308.

[5] B. Huang, Y. Yao and Z. Feng. “A Novel Wide Beam Dual-Band Dual-Polarization Stacked Microstrip Dielectric Antenna”. Microwave and Millimeter Wave Technology, 2007, pp. 1-4, April 2007. doi: http://dx.doi.org/10.1109/ICMMT.2007.381271.

[6] X. Sun, Z. Zhang and Z. Feng. “Dual-Band Circularly Polarized Stacked Annular-Ring Patch Antenna for GPS Application”. IEEE Antennas and Wireless Propagation Letters, Vol. 10, pp. 49-52, January 2011. doi: http://dx.doi.org/10.1109/LAWP.2011.2109365.

[7] R. K. Vishwakarma. “Design of rectangular stacked microstrip antenna for Dual-band”. International Conference on Emerging Trends and Photonic Devices & Systems, pp. 22-24, Dec. 2009. doi: http://dx.doi.org/10.1109/ELECTRO.2009.5441102.

[8] M. Noghabaei, S. K. A. Rahim and M. I. Sabran. “Dual Band Single Layer Microstrip Antenna with Circular Polarization for WiMAX Application”. 6th European Conference on Antennas and Propagation (EuCAP), pp. 1996-1999, March 2012. doi: http://dx.doi.org/10.1109/EuCAP.2012.6206490.

[9] F. Yang and Y. R. Samii. “A Single Layer Dual Band Circularly Polarized Microstrip Antenna for GPS Application”. IEEE Antennas and Propagation Society International Symposium, Vol. 4, pp. 720-723, 2002. doi: http://dx.doi.org/10.1109/APS.2002.1017084.

[10] Electronic Communication Committee, The European table of frequency allocations and applications in the frequency range 8.3 kHz to 3000 GHz (ECA TABLE), available at http://www.erodocdb.dk/docs/doc98/official/pdf/ERCRep025.pdf.

[11] L. S. Pereira, M. V. T. Heckler and C. Lucatel. “Design of Dual-Band and Dual-Polarized Microstrip Antenna for Applications on HAPs”. XXXIII Simpósio Brasileiro de Telecomunicações (SBrT’15), Juiz de Fora, MG, Brazil, September 1-4, 2015.

[12] D. M. Pozar, “Microwave Engineering”, John Wiley & Sons, 2011.

[13] Ansys Corporation, Ansys HFSS user’s guide, version 15.0, available at http://148.204.81.206/Ansys/readme.html.

Lucas Santos Pereira was born in São Luiz Gonzaga, Brazil, in 1990. He received the BSc. degree (2013) in Electrical Engineering (Emphasis in Electrical Power Systems) and the MSc. Degree in Electrical Engineering in 2014 (Emphasis in Energy Systems), both from Universidade Federal do Pampa, Alegrete, Brazil. He has been working as a teaching assistant at UNIPAMPA since 2013 in the field of Telecommunications Engineering. His current research interest is the design of dual-band microstrip antennas.

Marcos Vinício Thomas Heckler was born in Rio Grande, Brazil, in 1978. He received the BSc. Degree in Electrical Engineering (Emphasis in Electronics) in 2001 from Universidade Federal de Santa Maria – UFSM, Brazil, the MSc. Degree in Electronic Engineering (Microwaves and Optoelectronics) in 2003 from Instituto Tecnológico de Aeronáutica – ITA, Brazil, and the Dr.–Ing. Degree in Electrical Engineering in 2010 from Technische Universität München – TUM, Germany. From April to August 2003 he worked as a Research Assistant with the Antennas and Propagation Laboratory at ITA, Brazil. From October 2003 to June 2010 he worked as a Research Associate towards his PhD with the Antenna Group, Institute of Communications and Navigation, German Aerospace Center – DLR. He is currently a Professor at UNIPAMPA, in Alegrete, Brazil. His current research interests are the design of microstrip antennas and arrays, and the development of numerical techniques for microstrip antennas.

Cleiton Lucatel was born in Chapecó, Brazil, in 1982. He received the technical degree in Electromechanical (2001) from Serviço Nacional de Aprendizagem Industrial – SENAI, Chapecó, Brazil, and the technical degree in Electroelectronics (2008) from Centro Federal de Educação Tecnológica – CEFET, Chapecó, Brazil, and the technical degree in Industrial Automation (2012) from Colégio Técnico Industrial de Santa Maria – CTISM, Santa Maria, Brazil. He has been working as a member of the technical staff at UNIPAMPA since 2012.